Pet. Sci. (2016) 13:642–656
DOI 10.1007/s12182-016-0128-z

ORIGINAL PAPER

Formation of fine crystalline dolomites in lacustrine carbonates of the Eocene Sikou Depression, Bohai Bay Basin, East China

Yong-Qiang Yang[1] · Long-Wei Qiu[1] · Jay Gregg[2] · Zheng Shi[1] · Kuan-Hong Yu[1]

Received: 22 January 2016 / Published online: 7 November 2016

Abstract The genesis of the fine crystalline dolomites that exhibit good to excellent reservoir properties in the upper fourth member of the Eocene Shahejie Formation (Es_4^s) around the Sikou Sag, Bohai Bay Basin, is uncertain. This paper investigates the formation mechanisms of this fine crystalline dolomite using XRD, SEM, thin section analysis and geochemical data. The stratigraphy of the Sikou lacustrine carbonate is dominated by the repetition of metre-scale, high-frequency deposition cycles, and the amount of dolomite within a cycle increases upward from the cycle bottom. These dolomite crystals are 2–30 μm in length, subhedral to anhedral in shape and typically replace both grains and matrix. They also occur as rim cement and have thin lamellae within ooid cortices. Textural relations indicate that the dolomite predates equant sparry calcite cement and coarse calcite cement. The Sr concentrations of dolomites range from 900 to 1200 ppm. Dolomite $\delta^{18}O$ values (−11.3 to −8.2 ‰ PDB) are depleted relative to calcite mudstone (−8.3 to −5.4 ‰ PDB) that precipitated from lake water, while $\delta^{13}C$ values (0.06–1.74 ‰ PDB) are within the normal range of calcite mudstone values (−2.13 to 1.99 ‰ PDB). High $^{87}Sr/^{86}Sr$ values (0.710210–0.710844) indicate that amounts of Ca^{2+} and Mg^{2+} have been derived from the chemical weathering of Palaeozoic carbonate bedrocks. The high strontium concentration indicates that hypersaline conditions were maintained during the formation of the dolomites and that the dolomites were formed by the replacement of precursor calcite or by direct precipitation.

Keywords Dolomite · Lacustrine carbonate · Eocene · Sikou Sag · Bohai Bay Basin

1 Introduction

The controversy surrounding the origin of sedimentary dolomites is known as the "Dolomite Problem" (Van Tula 1916; Land 1985). Very fine crystalline dolomites are widely formed in varied types of lacustrine systems (Meister et al. 2011; Mauger and Compton 2011; Last et al. 2012; Casado et al. 2014; Meng et al. 2014a, b; Köster and Gilg 2015; Lu et al. 2015). They may form by replacement (dolomitization) of micrite matrix or allochems, or alternatively, they may occur as intraparticle and interparticle cements (Rosen and Coshell 1992). They consist of euhedral to anhedral crystals from a submicron size to 7 mm and are normally nonstoichiometric and poorly ordered (Last et al. 2012). Although the formation of fine dolomites in both modern and ancient lake records has been widely studied (Wright 1999; Bustillo et al. 2002; Casado et al. 2014; Lu et al. 2015), in many studies of lacustrine dolomites, there is insufficient evidence to determine whether the fine dolomite is of a primary or secondary (replacement) origin.

Fine crystalline dolomites are widely distributed at the Eocene lacustrine carbonate interval, in the Bohai Bay Basin (Jiang 2011; Peng 2011). Many previous studies have investigated the reservoir characteristics of lacustrine dolostones in the Bohai Bay Basin and have reported porosity improvement by the dolomitization (Xu 2013).

✉ Yong-Qiang Yang
yangyq_520@163.com

[1] School of Geosciences, China University of Petroleum, Qingdao 266580, Shandong, China

[2] Department of Geology, Oklahoma State University, Stillwater, OK 74075, USA

Edited by Jie Hao

However, the origin of dolomites is not as well documented, and the source of Mg^{2+} ions remains poorly resolved during the Es_4^s in the Bohai Bay Basin (Yuan et al. 2006). Understanding dolomite formation is a first step towards improved prediction of the architecture and distribution of dolomite reservoirs at regional scales.

In this study, the mineralogy, texture and stable isotope composition of minerals recovered from dolomites of the Sikou Sag, Bohai Bay Basin, are examined to better understand their origin. Carbon isotopes are used to determine the source of the carbonate ions, and strontium isotopes are used to determine the source of Ca^{2+} and Mg^{2+} ions. A detailed study of Sikou Sag dolomites may benefit strategies for lacustrine carbonate hydrocarbon exploration across the Bohai Bay Basin. This paper provides an example of early, high-frequency cyclic dolomite in lacustrine carbonate by high-salinity lake water.

2 Geological background

The Bohai Bay Basin, an important hydrocarbon-producing basin in China, is located on the eastern coast of China and covers an area of approximately 200,000 km^2. It is a complex rifted basin formed in the late Jurassic period through the early Tertiary period on the basement of the North China platform. The tectonic evolution of the Basin consists of a synrift stage (65.0–24.6 Ma) and a postrift stage (24.6 Ma to the present). The synrift stage can be further subdivided into an initial stage, an expansion stage, an expansion and deep subsidence stage, and a contraction stage. The sediments deposited at the synrift stage were restricted to the grabens and half grabens and were deposited in lacustrine environments. The postrift stage occurred during the deposition of the Guantao, Minghuazhen and Pingyuan Formations (Guo et al. 2010).

The Sikou Sag is located in the mid-western part of the Zhanhua Depression of the Bohai Bay Basin (Fig. 1a), which is adjacent to the Yihezhuang Uplift and bounded by the Yidong Fault (Pan and Li 2004). The northern part of the Sag is connected to the Chengdong Uplift; the western part of the sag is connected to the Yihezhuang Uplift through the Yidong Fault zone; the southern part is adjacent to the Chenjiazhuang Uplift bounded by the Gunan Fault zone, and the eastern part of the sag is connected to the Gudao Uplift and is also separated from the Bonan Sag by an east–west trending fault zone (Fig. 1b). In cross section, the research area can be divided into three parts: the Shaojia gentle ramp zone, the sag zone and the Yidong fault zone from the south-east to the north-west (Fig. 1c).

The Sikou Sag is filled by Cenozoic to Quaternary strata up to 5000 m thick in the depocentre. In ascending order, these strata consist of the Kongdian (Ek), Shahejie (Es), Dongying (Ed), Guantao (Ng), Minghuazhen (Nm) and Pingyuan (Qp) Formations. The Es formation can be further subdivided into four members, from the base to the top: Es_4, Es_3, Es_2 and Es_1 (Fig. 2). The Es_4 interval is the focus of this study. It ranges from 0 to 1400 m thick and consists of a lower "red bed" unit (Es_4^x: red interbedded sandstone and shale) and an upper grey mudstone interbedded with fine-grained carbonates and thin-bedded sandstones (Es_4^s). The Es_4 overlaps the Ek formation unconformably and is overlain in turn by the Es_3 Member, which is composed of 1000-m-thick brownish oil shales and dark-grey shales interbedded with thin sandstones and carbonates.

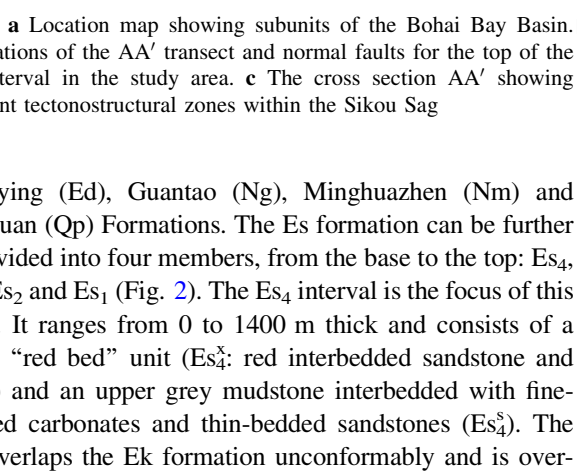

Fig. 1 **a** Location map showing subunits of the Bohai Bay Basin. **b** Locations of the AA′ transect and normal faults for the top of the Es_4^s interval in the study area. **c** The cross section AA′ showing different tectonostructural zones within the Sikou Sag

The study area began to subside during the deposition of the Es_4 Member resulting in a large topographic relief adjacent to the sag, which is steep in the north–south and gentle in the east–west directions. During this time interval, the climate was dry and warm, resulting in evaporative conditions. Sedimentary rocks in the study area consist of dark conglomerate, sandstone, shale, limestone, dolomite and gypsum beds ranging from 4.5 to 1735.5 m in thickness. Siliciclastic rocks dominate in the lower Es_4, whereas carbonate rock and gypsum are distributed in the upper Es_4. During the upper Es_4, there was mainly terrestrial detritus and carbonate deposition on the edge of the sag with gypsum, dark carbonate mudstone and shale deposited in the centre of the sag.

The Es_4^s Member of the Shahejie Formation in the Sikou Sag is interpreted as a complete marine third-order depositional sequence that formed during the rifting phase of the Bohai Bay Basin. Metre-scale, high-frequency depositional cycles are fundamental genetic units which make up the lacustrine carbonates in the Sikou Es_4^s interval. It reveals the extreme susceptibility of this system to high-frequency fluctuations in basin hydrology. The ideal high-frequency depositional cycles are characterized by a shallowing-upward trend of depositional facies and by a minor depositional unconformity at the top, which is related to subaerial exposure. A transgressive and regressive hemicycle can be observed within each genetic unit.

Three main facies associated with the research area are identified: (1) reef mounds are mainly developed along the downthrown block of the Yidong Fault, where algal bindstones are the main constituents. (2) Shoal facies developed on the gentle slope of the Shaojia area. These are composed of various grainstones and packstones. (3) The higher-salinity central-lake deposits of dark shale interbedded with gypsum and halite and thin dolomitized mudstone are mainly deposited at the centre of the lake. Deposition of these associations is interpreted to have taken place in a rift

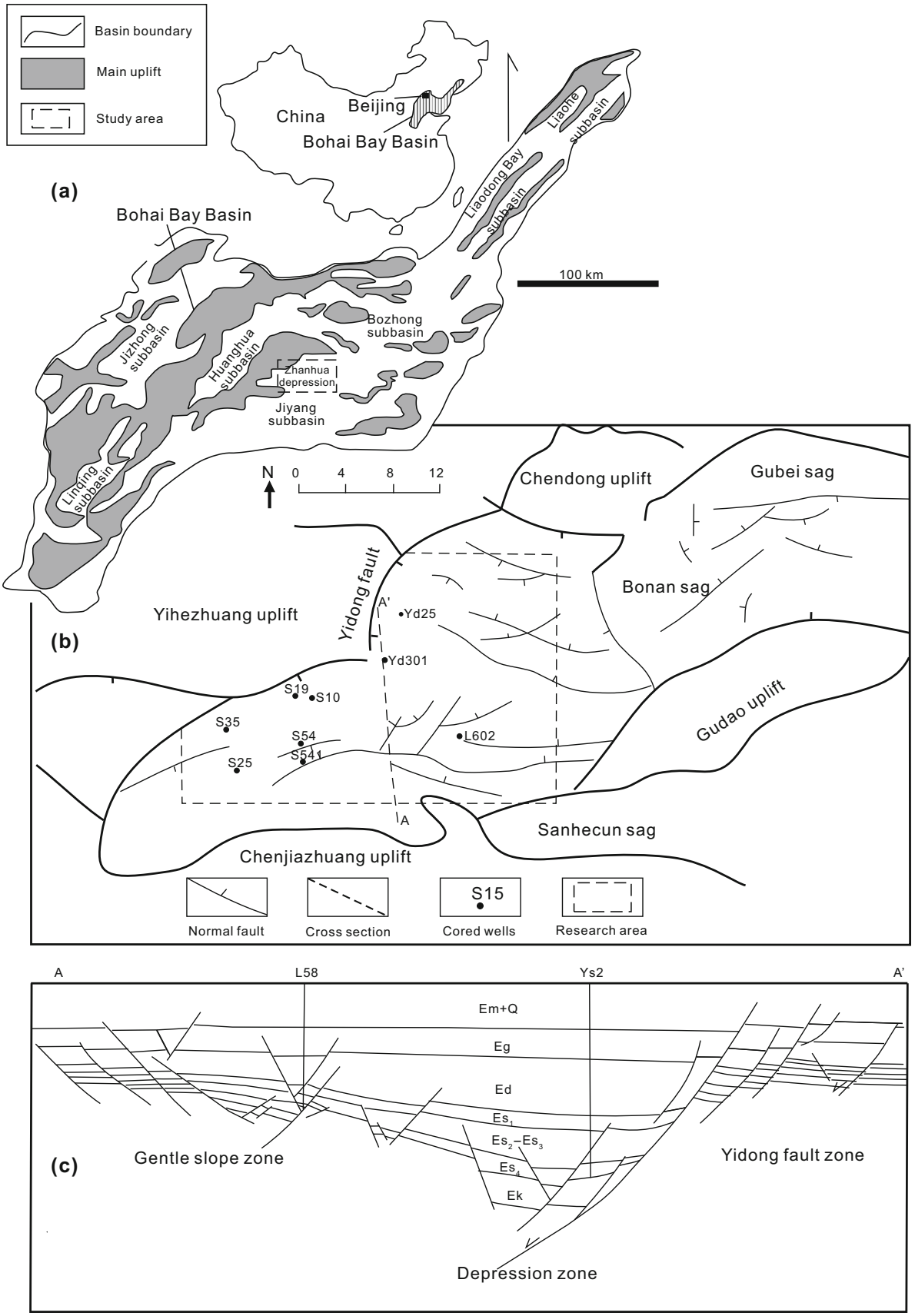
Basin boundary
Main uplift
Study area
China
Beijing
Bohai Bay Basin
(a)
Bohai Bay Basin
Liaodong Bay subbasin
Liaohe subbasin
100 km
Bozhong subbasin
Jizhong subbasin
Huanghua subbasin
Zhanhua depression
Jiyang subbasin
Linqing subbasin
N
0 4 8 12
Chendong uplift
Gubei sag
Yidong fault
Bonan sag
Yihezhuang uplift
(b)
A'
Yd25
Yd301
S19
S10
S35
S54
S541
S25
L602
Gudao uplift
A
Sanhecun sag
Chenjiazhuang uplift
Normal fault
Cross section
S15
Cored wells
Research area
A
L58
Ys2
A'
Em+Q
Eg
Ed
Es1
Es2–Es3
Es4
Ek
(c)
Gentle slope zone
Yidong fault zone
Depression zone

basin, where carbonate deposits changed to gypsum, halite and oil shale from the shore to the lake basin (Fig. 3). The sedimentation in the research area was dominantly controlled by wind-induced wave and wind action.

3 Data and methods

The petrographic characteristics of 52 polished thin sections were observed using a standard, transmitted light petrographic microscope. Staining with Alizarin red S and potassium ferricyanide differentiated between the ferroan and non-ferroan phases of calcite and dolomite. Twenty thin sections were studied with a CILT Mk5 cold-cathode luminoscope. The uncovered thin sections were exposed to electron radiation at 12 kV in a vacuum-sealed chamber that was attached to a Nikon Optiphot-pol petrographic microscope at Oklahoma State University. An FEI Quanta 600 F field emission scanning electron microscopy (SEM) at Oklahoma State University was used for SEM and energy-dispersive X-ray spectroscopy (EDS) of six dolomite samples. X-ray diffraction (XRD) analysis was carried out with powdered bulk rock materials on a Dmax 12 kW powder X-ray diffractometer. The samples were step-scanned at a 0°–70° 2θ interval.

Sample powders for chemical analysis were selected by the standard X-ray diffraction data and obtained from thin rock slabs using a dental drill. The strontium contents of dolomite were analysed by ICP-OES at Oklahoma State University. A total of 32 stable oxygen ($\delta^{18}O$) and carbon ($\delta^{13}C$) isotopes were analysed from powder dolomite and calcite samples using a Thermo Scientific Kiel IV automated carbonate device connected to a Thermo Scientific MAT253 dual-inlet isotope ratio mass spectrometer in the Analytical Laboratory for Paleoclimate Studies (ALPS) at the Jackson School of Geosciences, University of Texas at Austin. Dolomite and calcite powders were reacted with 100 % phosphoric acid at 90 °C using a Kiel III online carbonate preparation line connected to a ThermoFinnigan 252 mass spectrometer. Stable isotope ratios of carbonate samples are reported in per mil (‰) units VPDB. The long-term analytical precision based on >1500 stable isotopic determinations of a carbonate standard is ± 0.12 (2σ) for $\delta^{18}O$ and ± 0.06 (2σ) for $\delta^{13}C$. The Sr isotope ratio analysis of eight selected samples including dolomite and calcite was performed at Nanjing University using a VG Aldermaston Micromass 30 solid-source mass spectrometer.

4 Stratigraphic distribution

Fine crystalline dolomites are mainly found in various grainstones and packstones at all depths across the littoral to sublittoral zone, and a small proportion of very fine crystalline dolomite may also partially replace lime mudstone. The distribution and abundance of dolomites is closely related to the characteristics of metre-scale, high-frequency depositional cycles. Metre-scale, high-frequency depositional cycles are defined by integrating core-derived sedimentology data and well-log interpretations. They are the fundamental genetic units, which make up the lacustrine carbonates in the Es_4^s interval. A transgressive and regressive hemicycle can be observed within each genetic unit. The lower section of each transgressive hemicycle consists of low-energy lime mudstone (including shells), whereas the upper regressive hemicycle consists of higher-energy packstone and grainstone. The upper regressive facies are extensively dolomitized, whereas the lower transgressive facies are partially dolomitized or undolomitized (Fig. 4). The abundance of dolomite is proportional to the amount of precursor grain present in the rock.

5 Petrological characteristics

Two types of dolomite can be observed in the Sikou lacustrine carbonate: (1) fine crystalline dolomite (4–20 μm), which is dominantly grain-replacive, matrix-replacive and rim cement, represents approximately 95 % of all dolomite. (2) Medium crystalline dolomite occurring as cement in the interparticle porosity accounts for less than 5 %. The focus of this paper is on the first type of dolomite, which is positive for the reservoir quality of lacustrine carbonate.

In most grainy facies, including packstones and grainstones, fine crystalline dolomite has replaced both micrite and non-skeletal grains, which generally results in complete dolomitization (Fig. 5a), whereas the matrix of lime mudstone was partially dolomitized (Fig. 5b). The fossil fragments in the lime mudstone typically remained unaffected (Fig. 5c). Fine crystalline dolomite rhombs may also occur as isopachous cement filling intergranular pores (Figs. 5d, 7a). Most of the grains are composed of pure dolomite, but some ooids consist of alternating lamellae of calcite and dolomite (Fig. 5e). Variable proportions of slightly coarser dolomite rhombs "floating" in a very fine crystalline dolomite matrix can be observed in the research area (Fig. 5f).

All of the very fine crystalline dolomites in the matrix and grains exhibit dull red luminescence (Fig. 6a, b). The dolomite is associated with clay and anhydrite (Fig. 6c). The size of the fine dolomite crystals is 1–10 μm in length, and they are subhedral to anhedral in shape (Fig. 6d), and the dolomite formed a smooth interface due to two-dimensional nucleation growth (Fig. 6e, f). The very fine dolomite rhombs may partially or completely replace the intraclasts, algaes, ooids and peloids from outside to inside (Fig. 7).

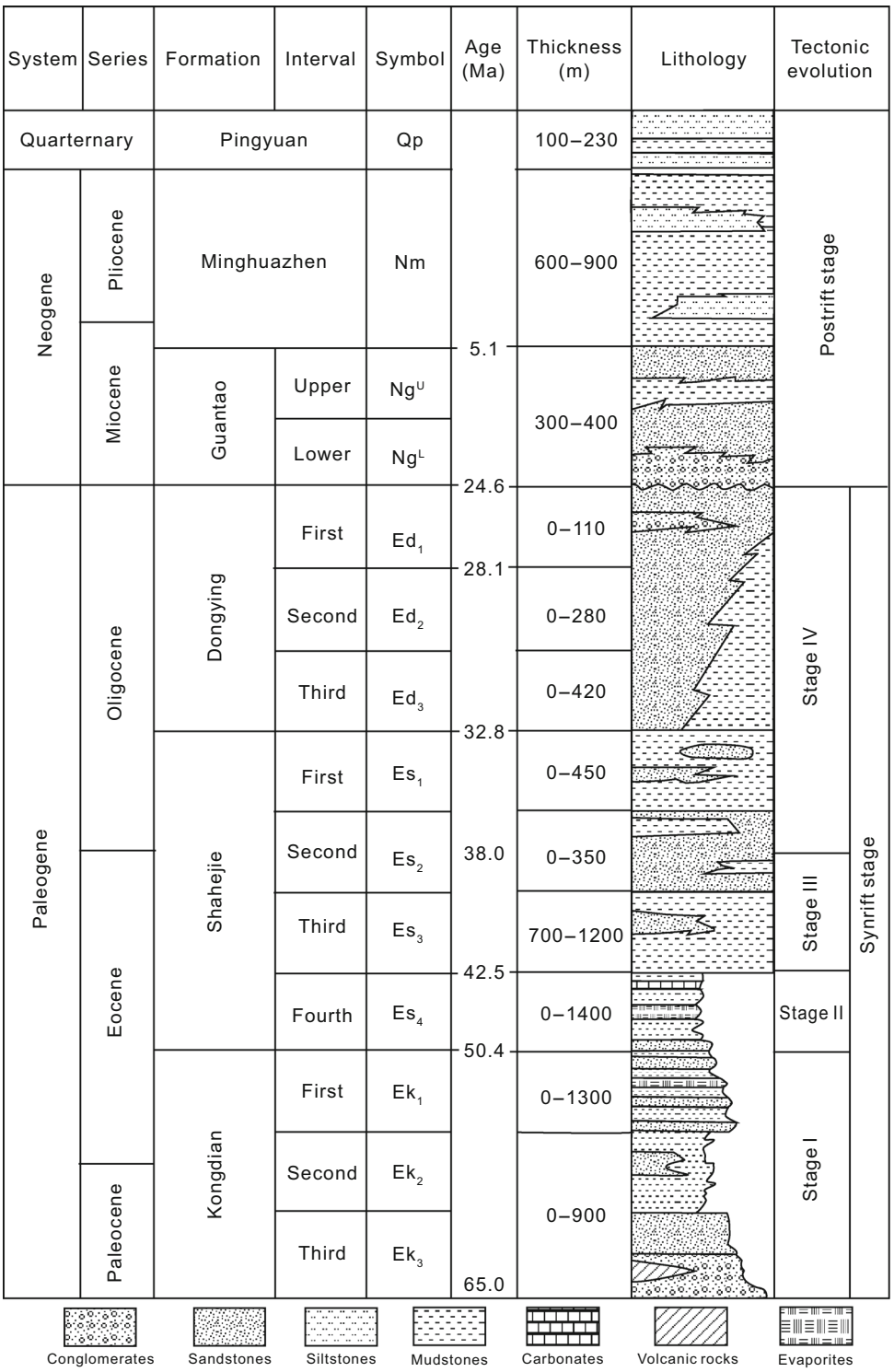

Fig. 2 Schematic Tertiary stratigraphy of the Sikou Sag in the Bohai Bay Basin (Guo et al. 2010)

6 Geochemistry

The $MgCO_3$ mol% of very fine dolomites ranges from 43 % to 50 %, with an average of 44.2 %. The strontium content in dolomites can generally be related to the texture or timing of formation. The strontium concentrations of fine dolomites range from 800 to 1200 ppm in the Sikou Sag.

Stable isotope analyses were carried out on samples of dolomites and calcites at different stratigraphic intervals

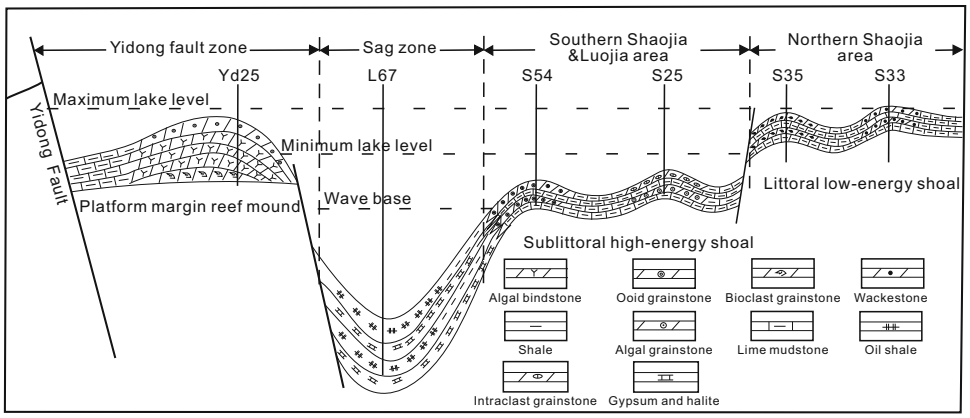

Fig. 3 Schematic model of the depositional distribution proposed for the lacustrine carbonate system of the upper Es_4^s in Paleogene interval around the Sikou Sag. See Fig. 1b for well locations

and lithofacies, and the results are shown in Table 1. The $\delta^{13}C$ values of calcites from lime mudstone range from −2.13 to 1.99 ‰ PDB during this time interval. The carbon isotope composition of dolomite ranges from approximately 0.06 to 1.74 ‰ PDB, which is consistent with the carbonate isotope composition of Es_4^s lacustrine water in the Sikou Sag (obtained from lime mudstone). The oxygen isotopic compositions of unaltered calcites from lime mudstone range from −8.3 to −5.4 ‰ PDB, while the oxygen isotopic compositions of fine crystalline dolomite range from −11.3 to −8.09 ‰ PDB.

The strontium isotope value of Eocene marine calcite was lower than 0.708000 (Veizer et al. 1999). The strontium isotope surrounding the Cambrian and Ordovician carbonate bedrock ranged from 0.7096 to 0.7140 (Liu et al. 2007). The strontium isotope signature of Sikou dolomites and calcite ranges from 0.710210 to 0.710844 and is significantly higher than the Eocene marine value, but this isotope signature is similar to the surrounding Cambrian and Ordovician carbonate bedrock.

7 Discussion and interpretation

7.1 Stratigraphic and petrographic considerations

Stratigraphic and petrographic observations indicated that very fine crystalline dolomite in the Sikou Sag is a product of penecontemporaneous or near-surface saline lake dolomitization. This interpretation is supported by the following lines of evidence:

1. In partially dolomitized metre-scale high-frequency cycles, the amount of dolomite within a metre-scale, shallowing-upward cycle increases upward from the cycle bottom. In the top grainy facies including packstones and grainstones, dolomite has replaced both micrite and non-skeletal grains generally resulting in complete dolomitization, whereas in the lower part, mudstones are dominated by calcite. These features illustrate that the dolomitization of the Es_4^s occurred during the formation of each cycle, and the high porosity in packstones and grainstones favours the dolomitization fluids flowing through.
2. Textural relations between the dolomite and other phases indicated that the very fine crystalline dolomite formed relatively early in the diagenetic history. Very fine crystalline dolomites clearly predate equant sparry calcite cement and coarse calcite cement, which commonly filled the intergranular pores and is interpreted as a shallow to medium burial phase. The very fine rim cement is interpreted as an early cement formed at the lake floor. The dolomite has replaced the grain and matrix, generally resulting in complete dolomitization. This may reflect the occurrence of subaqueous evaporative conditions over longer periods, as opposed to a shallow tidal flat depositional system which may have experienced intermittent "flushing" by dolomitizing fluids (Rott and Qing 2013).
3. The occurrence of very fine crystalline dolomite as rim cement and lamellae within dolomitized ooids of oolitic grainstone suggests very early, syndepositional formation of the dolomite either by direct precipitation from saline lake water or by dolomitization of precursor calcite. The alternation of dolomitized and undolomitized layers of coated grains was likely produced before complete ooid formation.
4. The dolomite pervasively replaces the grains of all facies, whereas the matrix is normally only partially affected. Pervasive replacement of the calcite by very fine, poorly ordered crystalline structures (Fig. 6d) has been documented in numerous examples in the

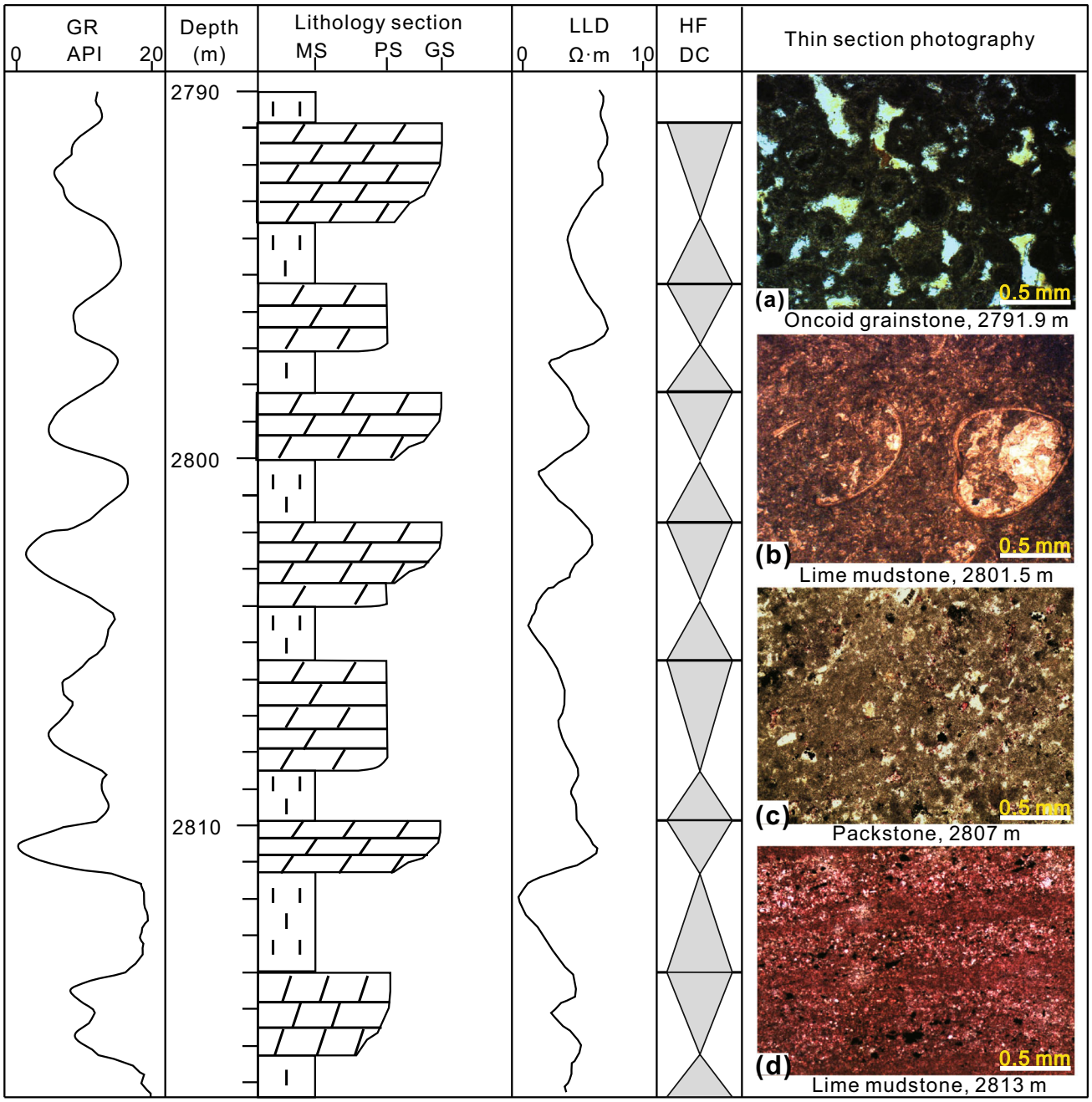

Fig. 4 High-frequency depositional cycles (HFDC) are recognized in the lacustrine strata, Well S54, the Sikou Sag. The amount of dolomites within a cycle increases upward from the cycle bottom. The *top part*, grainstone and packstone, of each cycle is completely dolomitized (*a*, *c*), whereas the *lower part* mudstones are dominated by calcite (*b*, *d*)

literature and is most often attributed to early diagenesis. In addition, some studies have shown that the dull red luminescence observed in dolomites (Fig. 6a, b) is commonly associated with early formed dolomites (Machel and Burton 1991). The crystal shape of dolomites is regulated only by the growth kinetics. At low temperatures, crystals grow by a layer-by-layer addition of atoms (Fig. 6e, f), resulting in faceted crystal sides (Sibley and Gregg 1987).

5. Based on petrographic observation, the euhedral dolomite rhombs are scattered throughout a very fine crystalline matrix and appear to overlap and cut across the finer crystals (Fig. 5f). They are interpreted as a product of recrystallization in its conventional sense, where dissolution–reprecipitation takes place on a micro-scale along crystal faces with concomitant increase in average crystal size (Malone et al. 1996; Rott and Qing 2013).

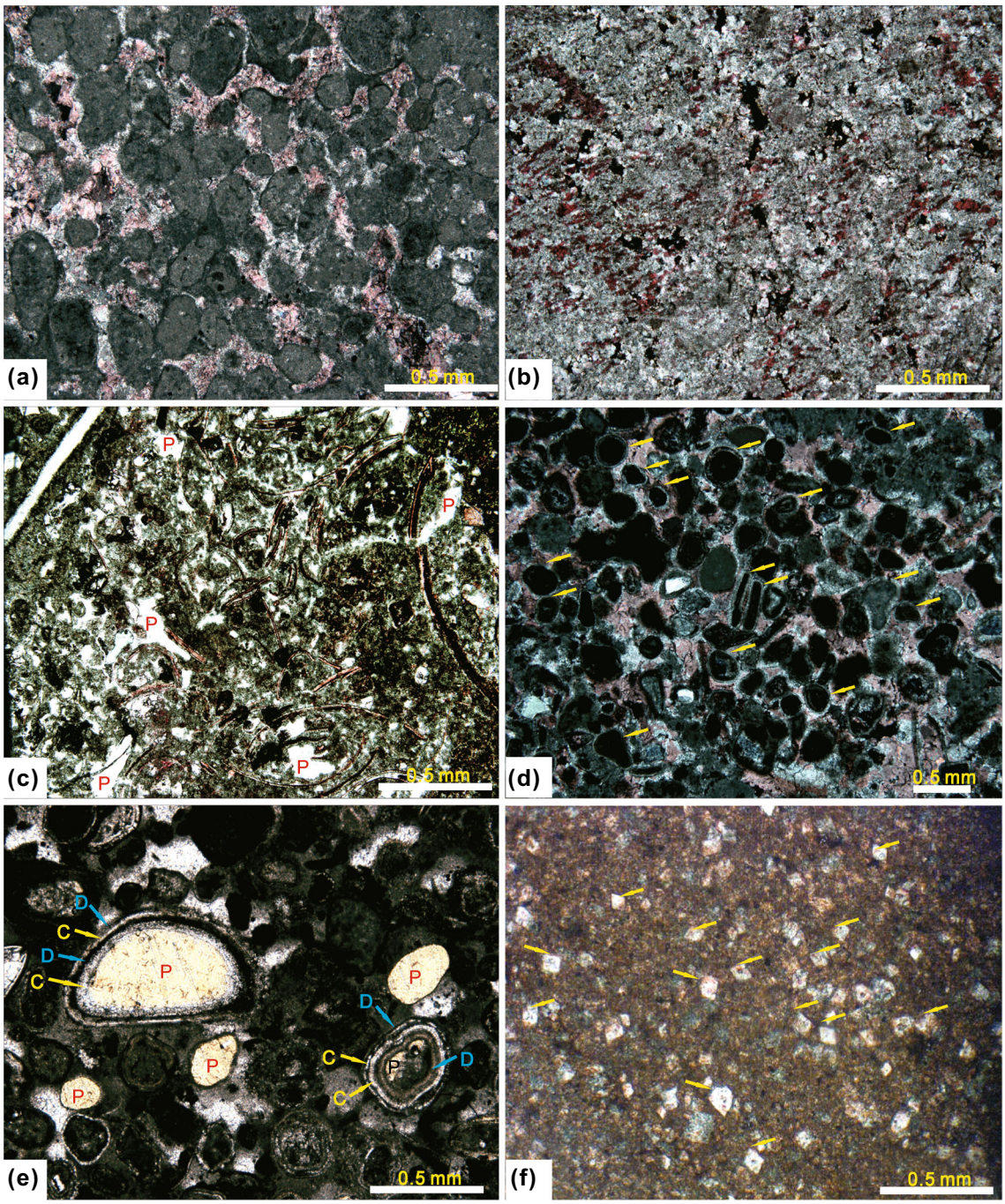

Fig. 5 Thin-section photomicrographs of fine crystalline dolomite. **a** Very fine dolomite in dolograinstone, the intergranular pores are filled by shallow-burial equant calcite cement, Well S541, depth 2681.6 m. **b** Partially dolomitized lime mudstone, Well Yd25, depth 3235.45 m. **c** Very fine dolomite in dolowackstone to packstone, undolomitized ostracoda shell fragments, Well S19, depth 2405.6 m. **d** Early isopachous dolomite cements, probably of lacustrine origin, in dolomitized grainstones, Well S54, depth 2798 m. **e** Pervasive dolomitized ooids with alternating lamellae of dolomite (*blue arrows*) and calcite (*yellow arrows*), parts of the core of ooids were dissolved. Well S25, depth 2318.7 m. **f** Euhedral, fine crystalline dolomite (*arrows*) scattered across very fine crystalline matrix in dolomitized limestone, Well S141, depth 2606.5 m. *Scale bars* are 0.5 mm

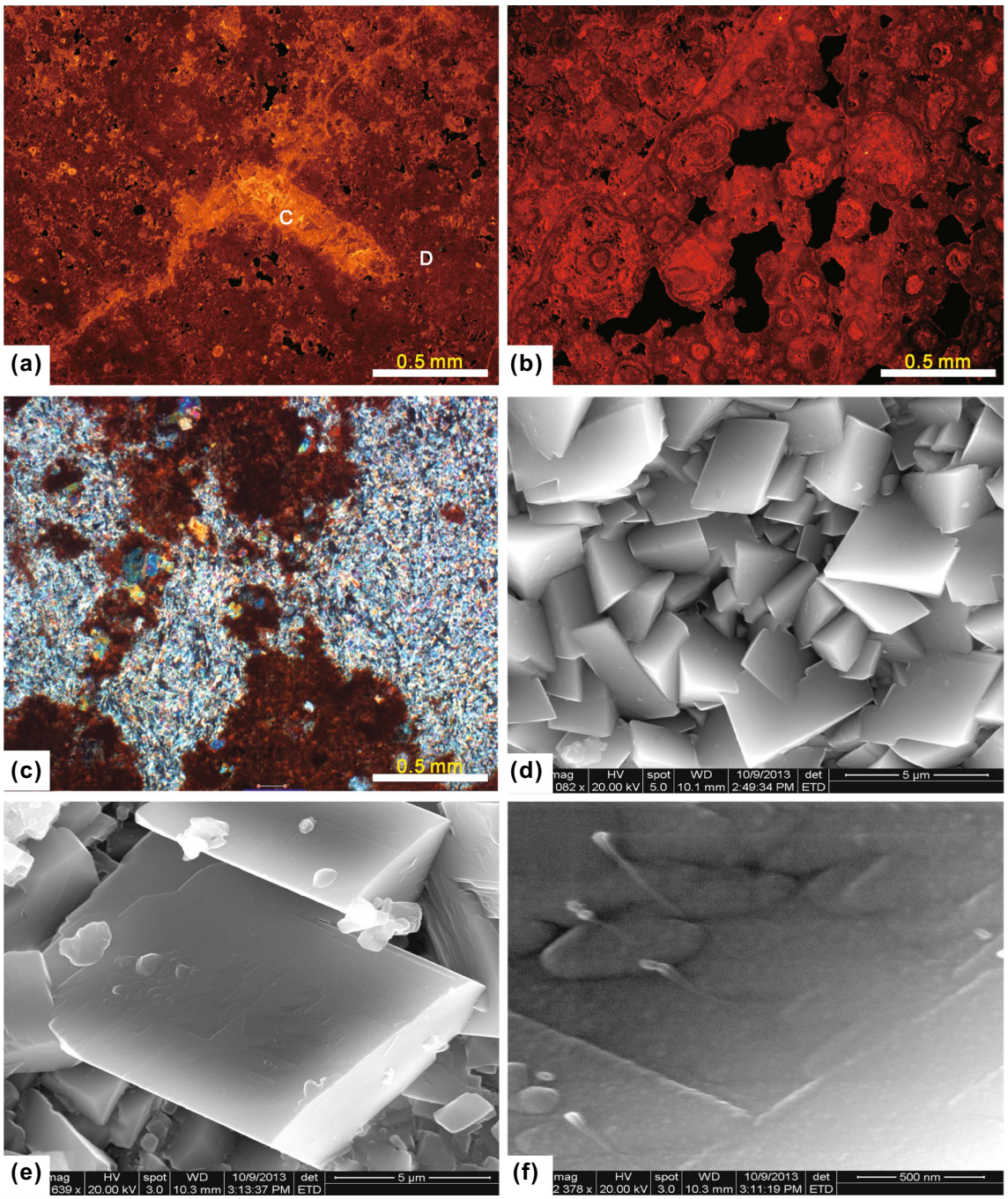

Fig. 6 **a** Cathodoluminescence photomicrograph of fine crystalline dolomite matrix (*dull red*) in packstone, Well Yd25, depth 3235.8 m. **b** Cathodoluminescence photomicrograph of fine crystalline dolomite grains (*dull red*) in oncoid grainstone, Well S54, depth 2796.52 m. **c** Nodular anhydrite cement in wackstone. Well Luo602, depth 2651.01 m. **d** SEM view of fine crystalline dolomite associated with clay in intraclastic grainstone. Well S541, depth 2181.6 m. **e**, **f** Planar dolomite forms a smooth interface due to two-dimensional nucleation growth. Well Yd25, depth 1890.4 m

7.2 Geochemical considerations

7.2.1 Source of Ca^{2+} and Mg^{2+} ions

Since the original studies of the upper fourth member of the Eocene Shahejie Formation in the Bohai Bay Basin, the source of Ca^{2+} and Mg^{2+} ions for the formation of lacustrine carbonate has been debated (Yuan et al. 2006)—is it marine or lacustrine in origin? There are four main processes cited in the literature that are beneficial to the lacustrine carbonate deposition in lakes. These include biogenic mediation, concentration through evaporation,

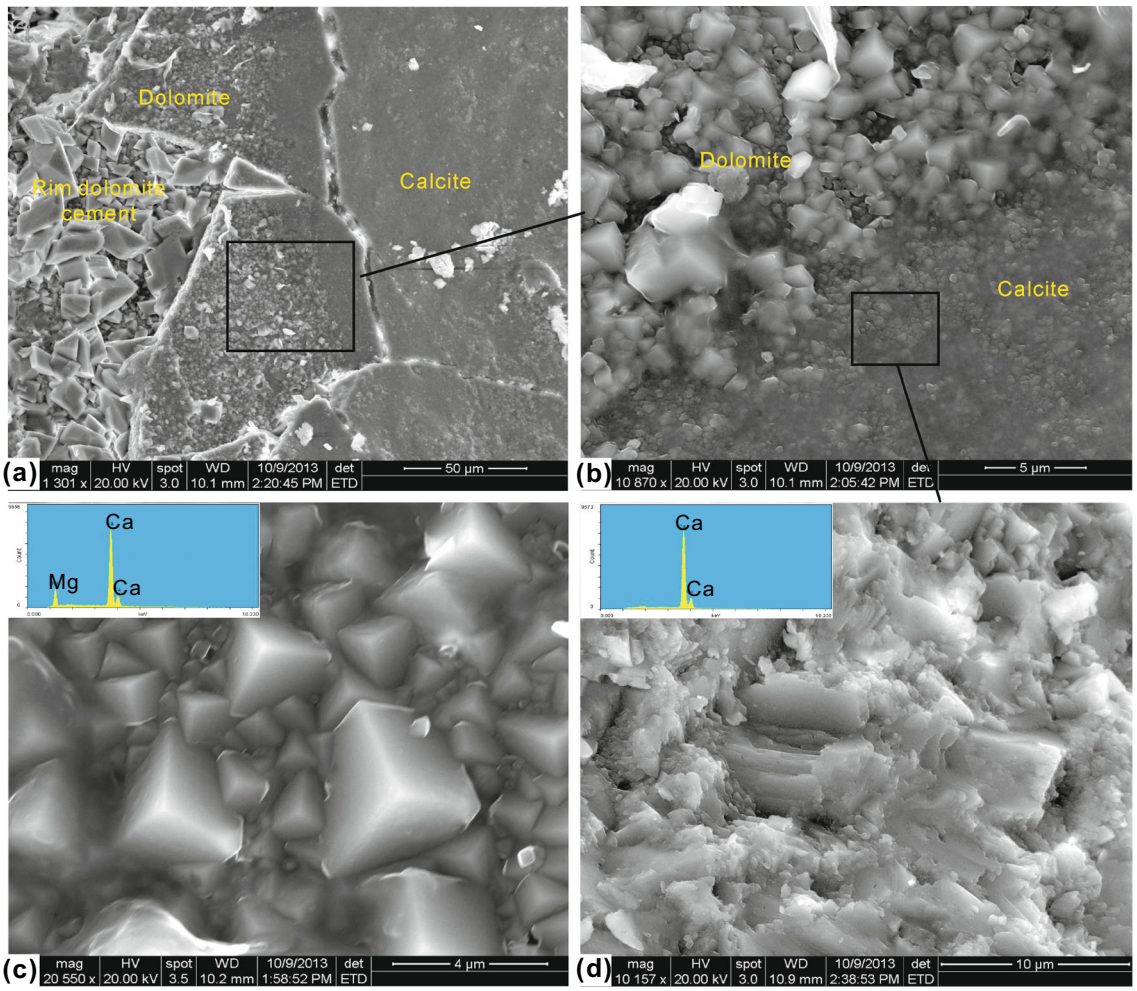

Fig. 7 SEM photomicrographs and EDX spectra of fine crystalline dolomites occurring as rim cements (**a**) and replacing the precursor grain from outside to inside (**b**, **c**, **d**). Well S25, depth 2318.7 m

waterborne clastic input and aeolian supply. The lake sediment type was controlled by the source rocks (Gebhardt et al. 2000). So the widespread carbonate rocks of the catchment area will allow for carbonate accumulations in the associated lake basin (Jones and Bowser 1978; Gierlowski-Kordesch 1998).

The carbon and oxygen stable isotopic composition of the sediments, suspended-load river input and the carbonate bedrock can be used to deduce the origins of lacustrine carbonate (Mauger and Compton 2011). The isotope values of bulk limestone samples indicate that the carbon and oxygen ratios of the Sikou carbonates differ significantly from the Eocene marine values, which range from $\delta^{13}C \approx 1.5$–2 ‰ VPDB and $\delta^{18}O \approx -1$ to 0 ‰ VPDB (Veizer et al. 1999).

The source of carbonate lacustrine sediments can be deduced from Sr isotopes. As strontium often substitutes for calcium, strontium isotopes can be used as a proxy to identify the source of the calcium; if the source of calcite is from marine water, then Sikou carbonate minerals would be expected to have a sea water $^{87}Sr/^{86}Sr$ ratio, which was lower than 0.708000 during the Eocene (Veizer et al. 1999). The $^{87}Sr/^{86}Sr$ ratio of the lime mudstones and dolomitized mudstones ranges from 0.7107 to 0.7113 and is significantly higher than the Eocene marine value, but is similar to the surrounding Cambrian and Ordovician carbonate bedrock, which ranges from 0.7096 to 0.7140 (Fig. 8). The planar distribution of the lacustrine carbonates during the upper fourth member of the Eocene Shahejie Formation was also controlled by the surrounding Palaeozoic carbonate bedrock in the Jiyang Sub-basin (Jiang 2011). All of these features indicate that the source of the Ca^{2+} and Mg^{2+} ions may come from chemical weathering of the surrounding carbonate bedrock and that the Sikou carbonate is of lacustrine origin.

7.2.2 *The formation environment of dolomites*

In general, later-diagenetic, coarsely crystalline dolomites have lower strontium concentration compared to the early

Table 1 Result of geochemical analysis of lacustrine carbonate samples

Well	Depth, m	Lithofacies	Sr, ppm	$\delta^{13}C$, ‰	$\delta^{18}O$, ‰	$^{87}Sr/^{86}Sr$
S10	2663	Lime mudstone	–	0.73	−7.28	–
S10	2669	Dolograinstone	1083	0.35	−8.49	–
S10	2672	Lime mudstone	–	1.52	−6.24	–
S10	2676	Lime mudstone	–	0.77	−5.85	–
S10	2683	Dolomud-wackstone	1207	1.29	−10.3	–
S10	2695	Lime mudstone	–	−1.77	−6.65	0.70990
S10	2695.5	Lime mudstone	–	−1.48	−7.83	–
S10	2698	Lime mudstone	–	−0.09	−8.16	0.71014
S10	2699	Dolomud-wackstone	–	2.04	−8.54	–
S10	2700	Lime mudstone	–	−0.32	−5.81	–
S10	2704.8	Dolomud-wackstone		−2.10	−8.25	–
S10	2705	Lime mudstone	–	−2.1	−8.25	–
S13	2802	Dolomud-wackstone	971	1.74	−11.1	–
S13	2818	Dolomud-wackstone	939	0.57	−9.09	–
S141	2542.4	Dolomud-wackstone	–	−0.94	−8.42	–
S141	2607	Lime mudstone	–	−0.69	−8.10	–
S141	2609	Lime mudstone	–	−0.94	−8.11	–
S19	2403	Lime mudstone	–	−0.77	−8.19	0.71047
S19	2409	Lime mudstone	–	−2.13	−6.37	–
S25	2318.7	Dolograinstone	1102	0.92	−9.72	0.71042
S54	2428.3	Lime mudstone	–	−1.48	−7.83	0.71048
S54	2804.6	Dolograinstone	–	−1.75	−9.52	–
S541	2674	Dolograinstone	901	1.43	−8.76	0.70964
S541	2681.6	Dolograinstone	1081	0.06	−8.09	–
Yd25	3226.6	Dolograinstone	1205	1.14	−9.67	–
Yd25	3238	Lime mudstone	–	0.29	−7.38	–
Yd25	3235	Dolograinstone	1127	0.13	−11.02	0.70981
Yd25	3245	Lime mudstone	–	0.69	−6.63	–
Yd301	3590.3	Dolograinstone	–	2.06	−10.20	–
Yd301	3592.8	Dolograinstone	–	2.20	−9.88	–
Yd301	3593.3	Dolograinstone	1194	1.61	−10.62	0.71045
Yd301	3596	Lime mudstone	–	2.29	−6.65	–

fine crystalline dolomites (Hu et al. 2013). High strontium concentrations (more than 1000 ppm) occur in dolomites precipitated from intensively evaporated waters and from dolomitizing fluids with high Sr/Ca ratios (Morrow 1990). The strontium concentrations of fine crystalline dolomites ranged from 800 to 1200 ppm in the Sikou Sag, indicating that the fine dolomites formed in intensively evaporated waters (Table 1).

C–O isotopic compositions of dolomites are mainly affected by temperature and salinity in the medium. Carbon isotopic composition is influenced by different sources of carbon, while oxygen isotopic fractionation occurs during the evaporation of water as temperature rises (Yang et al. 2013). Overall, the $\delta^{18}O$ PDB and $\delta^{13}C$ PDB values become greater with increasing salinity (Lu et al. 2015). The dolomite in the Sikou Sag may have undergone alteration by diagenetic fluids, and as a result, the oxygen isotopic signature was reset; however, the carbon was not affected (Fig. 9). As the isotope fractionation between calcites and coevally precipitated dolomite is approximately 2.5 ‰ (Swart and Melim 2000; Wang et al. 2012), the $\delta^{18}O$ values of dolomite should be slightly higher than $\delta^{18}O$ values of calcite, if they formed from the same lacustrine water. However, the $\delta^{18}O$ values of dolomites from the Sikou Sag are significantly lower than the predicted values for dolomites derived from Es_4^s lacustrine water. The previous textural relations reveal that the initial calcite precursors were replaced relatively early by fine crystalline dolomite. Owing to the fluctuation of lake levels, the early formed dolomites were always affected by the meteoric water, and formed mouldic and vuggy pores (Figs. 5e, 6b), and caused a negative shift of the oxygen isotopic value of the early formed dolomites (Fig. 9).

7.3 Mechanism of dolomite formation

Owing to seasonal evaporation, carbonate mainly formed inshore, while gypsum and halite occurred at the centre of the lake in most of the modern and ancient saline lakes (Peng 2011; Mauger and Compton 2011). The existence of wet/dry cycles in surficial environments seems to be an essential requirement for the nucleation of dolomites (Deelman 2003). Based on the distribution of dolomites in high-frequency depositional cycles, the formation process of fine dolomite in the Sikou Sag was interpreted to undergo two stages of evolution (Fig. 10).

Early brackish lake stage: This stage represents the most humid interval, in which the lake level is high. The chemical weathering of Cambrian and Ordovician carbonate bedrock produces Ca^{2+}, Mg^{2+} and HCO^{3-} ions which are transported to the Sikou Sag by run-off or through flow. The sulphate reduction began at the centre of the sag, where it is likely anoxic and stratified (Mauger and Compton 2011). Early evaporation causes salinities to increase over time, and calcite is the least soluble of the major salts. As a result, it will precipitate in the shallow-water zone during evaporation, while the organic mudstone deposits occurred at the centre of the lake.

Late saline lake stage: This stage represents the aridity interval, and the greater evaporation rates resulted in the low lake level and the increase in salinity. The increase in the Mg/Ca ratio, following the removal of Ca^{2+} during gypsum precipitation, favours precipitation of Mg calcite. As the Mg/Ca ion ratio of the pore waters rises further, fine crystalline dolomite may replace existing calcite and high-Mg calcite.

The fine dolomite occurring in the grains and the matrix is interpreted to signify an early replacement origin, which is

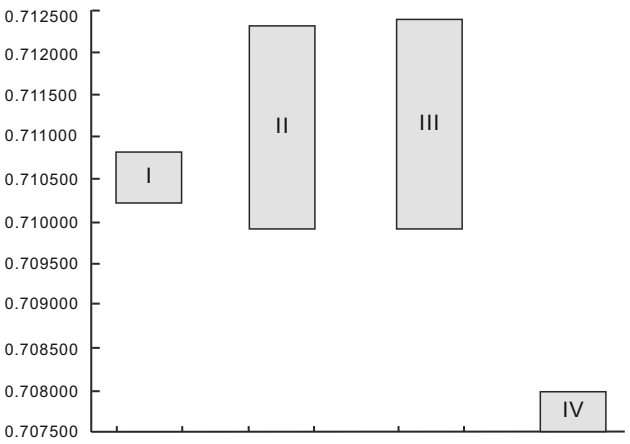

Fig. 8 $^{87}Sr/^{86}Sr$ isotope plot of different samples, *I* is from the samples in the Sikou Sag; *II* and *III* represent the surrounding Cambrian and Ordovician carbonate bedrock (Liu et al. 2007); *IV* represents the Eocene marine values (Veizer et al. 1999)

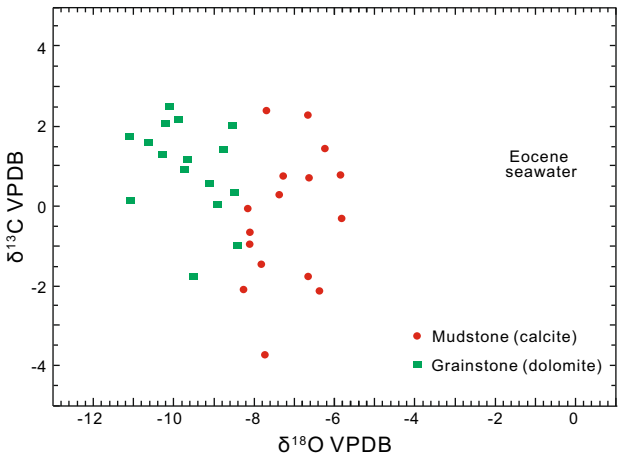

Fig. 9 $\delta^{13}C$ and $\delta^{18}O$ values of fine crystalline dolomites and calcites from Sikou lacustrine carbonates. Values are displayed in standard delta notation relative to the PDB standard. Expected $\delta^{13}C$ and $\delta^{18}O$ ranges of primary calcite precipitated from Eocene seawater (Veizer et al. 1999)

proven by the existence of the replacement (Fig. 7) and the coexistence of calcite and dolomite in the matrix (Fig. 5b, c). According to the early replacement origin, the fine dolomite may replace the tiny calcite crystals covering the grains during the increase in salinity in the lake water. It is likely that higher-magnesium calcite lamellae with higher microporosity are more prone to dolomitization than the lower-magnesium calcite lamellae, which formed the alternating lamellae of calcite and dolomite in the ooids (Rott and Qing 2013). However, replacement was not observed at the thin dolomite lamellae contained within some ooids.

The formation of lamellae and cement is considered in the published literature as primary dolomite in response to changing chemical conditions (Mitchell et al. 1987; Mazzullo et al. 1995). The precipitation of primary dolomites from modern and ancient lacustrine environments has been widely documented in the literature (De Deckker and Last 1988; Arenas et al. 1999). Some of the fine dolomite cement was also interpreted to be of primary origin in a shallow lacustrine environment (Mazzullo 2000). Two main models have been established for the primary very fine lacustrine dolomite. Firstly, the bacterial removal of sulphate and resultant increase in availability of Mg^{2+} ions made the very fine dolomite directly precipitate from the evaporating lake waters (Burn et al. 2000). Secondly, Meister et al. (2011) reported that fine-grained dolomite probably precipitates directly in the well-aerated water column from highly alkaline brine, whereas microbial alkalinity production and pH increases are negligible. So the precipitation of dolomites from saline lake water should be considered in light of the possible origin of very fine rim cement and dolomite lamellae within ooids in the Sikou Sag, and inferring a similar genesis for the origin of

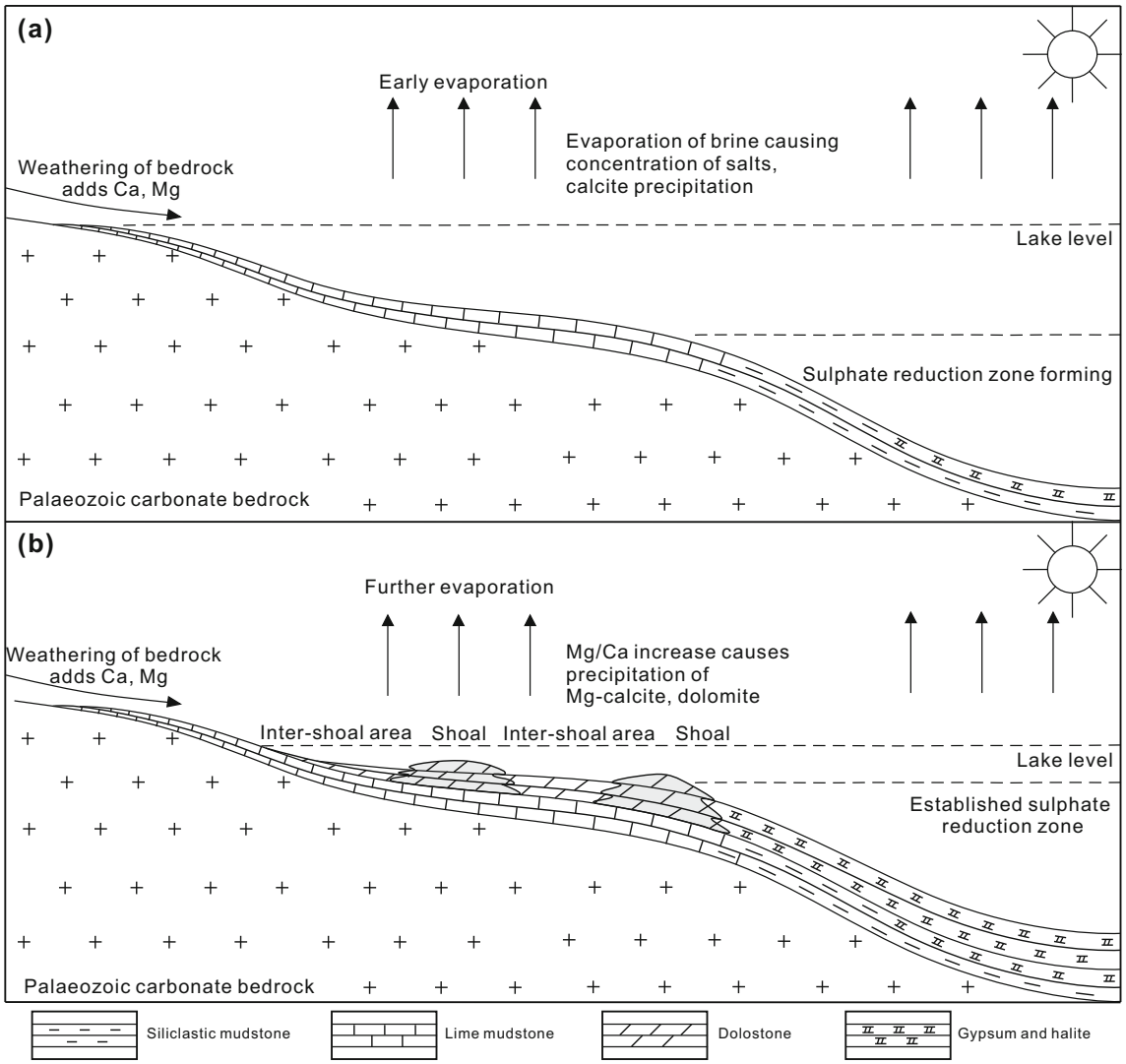

Fig. 10 Proposed mechanism of dolomitization for the upper fourth member of the Eocene Shahejie Formation (Es_4^s) around the Sikou Sag. **a** Saline lake with moderate salt and calcite precipitation during early stages of salt accumulation; **b** further evaporation elevated Mg/Ca ratios and sulphate reduced, which led to dolomite precipitation and replaced the precursor calcite

dolomite mud should also be explored in dolomitized mudstone.

7.4 Impact on development of hydrocarbon reservoir

Many previous studies have reported the porosity improvement by dolomitization (Moore 2001; Swei and Tucker 2012; Meng et al. 2014a, b). In this context, in most grainy facies and mudstones, fine crystalline dolomite has replaced both micrite and non-skeletal grains, generally resulting in a significant increase in reservoir quality, particularly permeability, compared with the precursor limestone (Xu 2013). With the development of intercrystalline pores, dolomites are more resistant to burial-related effects which therefore cause little reduction in porosity relative to limestones (Rabbani 2004) and are more frequently affected by fracturing than limestones and sandstones (Sun 1995). In addition, the intercrystalline pores provided conduits for the influx of hydrocarbons and acidic fluids, enhancing porosity due to leaching.

8 Conclusions

The upper fourth member of the Eocene Shahejie Formation in the Sikou Sag consists of abundant grain- and matrix replacement very fine crystalline dolomite (2–30 μm). The dolomite is interpreted as a product of near-surface dolomitization of precursor calcite by lacustrine water of high salinity. Similar to the surrounding Cambrian and Ordovician bedrock strontium isotope

values, the dolomite and calcite support a carbonate bedrock source for some of the Ca and Mg delivered to the sag. In particular, the chemical weathering of carbonate bedrock may raise the Mg/Ca ratios of the lacustrine waters to achieve the high Mg/Ca ratios required for dolomite precipitation. Most of the dolomite crystals typically replace precursor grains and matrix. However, the direct precipitation of dolomites from evaporating lake waters should be considered in light of the possible origin of very early rim dolomite cement and dolomite lamellae within ooids.

Acknowledgments This work was supported by the National Basic Research Program of China (Grant No. 2014CB239002) and Natural Science Foundation of Shandong Province, China (Grant No. ZR2014DQ016). The China University of Petroleum (East China) provided facilities for this research. The authors thank the Hekou Production Factory of the Shengli Oil Field Company for some data preparation.

References

Arenas C, Alonso Zarza AM, Pardo G. Dedolomitization and other diagenetic processes in Miocene lacustrine deposits, Ebro Basin (Spain). Sediment Geol. 1999;125:23–45.

Burn SJ, McKenzie JA, Vasconcelos C. Dolomite formation and biogeochemical cycles in the Phanerozoic. Sedimentology. 2000;47(s1):49–61.

Bustillo MA, Arribas ME, Bustillo M. Dolomitization and silicification in low-energy lacustrine carbonates (Paleogene, Madrid Basin, Spain). Sediment Geol. 2002;151:107–26.

Casado AI, Alonso-Zarza AM, La Iglesia A. Morphology and origin of dolomite in paleosols and lacustrine sequences. Examples from the Miocene of the Madrid Basin. Sediment Geol. 2014;312:50–62.

De Deckker P, Last WM. Modern dolomite deposition in continental, saline lakes, western Victoria, Australia. Geology. 1988;16:29–32.

Deelman JC. Low-temperature formation of dolomite and magnesite. Eindhoven: CD Publications; 2003. p. 504.

Gebhardt U, Merkel T, Szabados A. Karbonatsedimentation in siliziklastischen fluviatilen Abfolgen. Freib Forsch. 2000;490:133–68.

Gierlowski-Kordesch EH. Carbonate deposition in an ephemeral siliciclastic alluvial system: Jurassic Shuttle Meadow Formation, Newark Supergroup, Hartford Basin, U.S.A. Palaeogeogr Palaeoclimatol Palaeoecol. 1998;140:161–84.

Guo X, He S, Liu K, et al. Oil generation as the dominant overpressure mechanism in the Cenozoic Dongying Depression, Bohai Bay Basin, China. AAPG Bull. 2010;94:1859–81.

Hu ZW, Huang SJ, Li ZM, et al. Geochemical characteristics of the Permian Changxing Formation reef dolomites, northeastern Sichuan Basin, China. Pet Sci. 2013;10(1):38–49.

Jiang XL. Main controlling factors of lacustrine carbonate rock in Jiyang Depression. Pet Geol Recovery Effic. 2011;18:23–7 **(in Chinese)**.

Jones BF, Bowser CJ. The mineralogy and related chemistry of lake sediments. In: Lerman A, editor. Lakes: chemistry, geology, physics. Springer: Berlin; 1978. p. 179–235.

Köster MH, Gilg HA. Pedogenic, palustrine and groundwater dolomite formation in non-marine bentonites (Bavaria, Germany). Clay Miner. 2015;50(2):163–83.

Land LS. The origin of massive dolomite. J Geol Educ. 1985;33:112–25.

Last FM, Last WM, Halden NM. Modern and late Holocene dolomite formation: Manito, Saskatchewan, Canada. Sediment Geol. 2012;281:222–37.

Liu SG, Shi HX, Wang GZ, et al. Formation mechanism of Lower Paleozoic carbonate reservoirs in Zhuanghai Buried Hill. Nat Gas Ind. 2007;27(10):1–5 **(in Chinese)**.

Lu XC, Shi JA, Zhang SC, et al. The origin and formation model of Permian dolostones on the northwestern margin of Junggar Basin, China. J Asian Earth Sci. 2015;105:456–67.

Machel HG, Burton EA. Factors governing cathodoluminescence in calcite and dolomite and their implications for studies of carbonate diagenesis. In: Barker CE, Kopp OC, editors. Luminescence microscopy and spectroscopy: qualitative and quantitative applications: SPEM, short course; 1991. vol. 25, p. 37–57.

Malone MJ, Baker PA, Burns SJ. Recrystallization of dolomite: an experimental study from 50–200 °C. Geochim Cosmochim Acta. 1996;60:2189–207.

Mauger CL, Compton JS. Formation of modern dolomite in hypersaline pans of the Western Cape, South Africa. Sedimentology. 2011;58:1678–92.

Mazzullo SJ, Bischoff WD, Teal CS. Holocene subtidal dolomitization, north Belize. Geology. 1995;23:341–4.

Mazzullo SJ. Organogenic dolomitization in peritidal to deep-sea sediments. J Sediment Res. 2000;70:10–23.

Meister P, Reyes C, Beaumont W, et al. Calcium and magnesium-limited dolomite precipitation at Deep Springs Lake, California. Sedimentology. 2011;58:1810–30.

Meng WB, Wu HZ, Li GR, et al. Dolomitization mechanisms and influence on reservoir development in the Upper Permian Changxing Formation in Yuanba area, northern Sichuan Basin. Acta Pet Sin. 2014a;30(3):699–708.

Meng Y, Zhu HD, Li XN, et al. Thermodynamic analyses of dolomite dissolution and prediction of the zones of secondary porosity: a case study of the tight tuffaceous dolomite reservoir of the second member, Permian Lucaogou Formation, Santanghu Basin, NW China. Pet Explor Dev. 2014b;41(6):754–60 **(in Chinese)**.

Mitchell JT, Land LS, Miser DE. Modern marine dolomite cement in a north Jamaican fringing reef. Geology. 1987;15:557–60.

Moore CH. Carbonate reservoirs. Developments in sedimentology, vol. 55. Amsterdam: Elsevier; 2001. p. 444.

Morrow DW. Dolomite, part 2: dolomitization models and ancient dolostones. In: McIlreath IA, Morrow DW, editors. Diagenesis. Geoscience Canada repint series 4; 1990. p. 125–39.

Pan YL, Li S. Large-scale continental rift basin sequence stratigraphy and subtle oil and gas reservoirs: a case study in the Jiyang Sag. Beijing: Petroleum Industry Press; 2004. p. 57 **(in Chinese)**.

Peng CS. Distribution of favorable lacustrine carbonate reservoirs: A case from the Upper Es_4 of Zhanhua Sag, Bohai Bay Basin. Pet Explor Dev. 2011;38(4):435–43 **(in Chinese)**.

Rabbani AR. Geochemical and petrographical study of dolomite facies in the Dalan and Kangan gas reservoirs in the south of Iran. Res Sci Eng Pet Bull. 2004;14(49):34–46.

Rosen MR, Coshell L. A new location of Holocene dolomite formation, Lake Hayward, Western Australia. Sedimentology. 1992;39:161–6.

Rott CM, Qing H. Early dolomitization and recrystallization in shallow marine carbonates, Mississippian Alida beds, Willistone Basin (Canada): evidence from petrography and isotope geochemistry. J Sediment Res. 2013;83:928–41.

Sibley DF, Gregg JM. Classification of dolomite rock textures. J Sediment Res. 1987;57:967–75.

Sun SG. Dolomite reservoirs: porosity evolution and reservoir characteristic. AAPG Bull. 1995;79(21):186–204.

Swart PK, Melim L. The origin of dolomites in Tertiary sediments from the margin of Great Bahama Bank. J Sediment Res. 2000;70:738–48.

Swei GH, Tucker ME. Impact of diagenesis on reservoir quality in ramp carbonates: Gialo formation (Middle Eocene), Sirt Basin, Libya. J Pet Geol. 2012;35(1):25–48.

Van Tula FM. The present status of the dolomite problem. Science. 1916;44:688–90.

Veizer J, Ala D, Azmy K, et al. $^{87}Sr/^{86}Sr$, $\delta^{13}C$ and $\delta^{18}O$ evolution of Phanerozoic seawater. Chem Geol. 1999;161:59–88.

Wang SQ, Zhao L, Cheng XB, et al. Geochemical characteristics and genetic model of dolomite reservoirs in the eastern margin of the Pre-Caspian Basin. Pet Sci. 2012;2:161–9.

Wright DT. The role of sulphate reducing bacteria and cyanobacteria in dolomite formation in distal ephemeral lakes of the Coorong region, South Australia. Sediment Geol. 1999;126:147–57.

Xu L. Effects of dolomitization in carbonate rocks on reservoir porosity in the Dongying Depression. Bull Mineral Petrol Geochem. 2013;32:463–7 **(in Chinese)**.

Yang ZH, Zhang N, Dong JX, et al. Carbon oxygen isotope analysis and its significance of carbonate in the Zhaogezhuang Section of Early Ordovician in Tangshan, North China. J Earth Sci. 2013;24(6):918–34.

Yuan WF, Chen SY, Zeng C. Study on marine transgression of Palaogene Shahejie Formation in Jiyang Depression. Acta Pet Sin. 2006;27:40–9 **(in Chinese)**.